JVI Journals.ASM.org

Dynasore Disrupts Trafficking of Herpes Simplex Virus Proteins

Mascha B. Mues,[a*] Natalia Cheshenko,[b] Duncan W. Wilson,[c] Leslie Gunther-Cummins,[d] Betsy C. Herold[b,d]

Departments of Medicine,[a] Pediatrics,[b] Developmental and Molecular Biology,[c] and Microbiology and Immunology,[d] Albert Einstein College of Medicine, Bronx, New York, USA

ABSTRACT

Dynasore, a small-molecule inhibitor of the GTPase activity of dynamin, inhibits the entry of several viruses, including herpes simplex virus (HSV), but its impact on other steps in the viral life cycle has not been delineated. The current study was designed to test the hypothesis that dynamin is required for viral protein trafficking and thus has pleiotropic inhibitory effects on HSV infection. Dynasore inhibited HSV-1 and HSV-2 infection of human epithelial and neuronal cells, including primary genital tract cells and human fetal neurons and astrocytes. Similar results were obtained when cells were transfected with a plasmid expressing dominant negative dynamin. Kinetic studies demonstrated that dynasore reduced the number of viral capsids reaching the nuclear pore if added at the time of viral entry and that, when added as late as 8 h postentry, dynasore blocked the transport of newly synthesized viral proteins from the nucleus to the cytosol. Proximity ligation assays demonstrated that treatment with dynasore prevented the colocalization of VP5 and dynamin. This resulted in a reduction in the number of viral capsids isolated from sucrose gradients. Fewer capsids were observed by electron microscopy in dynasore-treated cells than in control-treated cells. There were also reductions in infectious progeny released into culture supernatants and in cell-to-cell spread. Together, these findings suggest that targeting dynamin-HSV interactions may provide a new strategy for HSV treatment and prevention.

IMPORTANCE

HSV infections remain a global health problem associated with significant morbidity, particularly in neonates and immunocompromised hosts, highlighting the need for novel approaches to treatment and prevention. The current studies indicate that dynamin plays a role in multiple steps in the viral life cycle and provides a new target for antiviral therapy. Dynasore, a small-molecule inhibitor of dynamin, has pleiotropic effects on HSV-1 and HSV-2 infection and impedes viral entry, trafficking of viral proteins, and capsid formation.

Herpes simplex viruses 1 and 2 (HSV-1 and HSV-2) are epidemic worldwide, and epidemiological studies consistently demonstrate that HSV-2 infection is associated with an increased risk of HIV acquisition and transmission, further fueling the HIV epidemic (1–3). Acyclovir and related prodrugs, which inhibit viral DNA replication, are effective at treating HSV disease but do not eradicate the virus or prevent viral reactivation, and resistance has emerged as a clinical problem (1). Suppressive dosing reduces clinical recurrences and subclinical viral shedding (4) but has had little impact on HIV transmission or acquisition in large-scale clinical trials (5–7). These epidemiological findings underscore the need to identify additional biomedical strategies for HSV prevention and treatment.

The earliest pharmacological approach to HSV prevention focused on developing drugs to block viral entry. Several sulfated or sulfonated polymers, which competitively blocked the binding of HSV-1 and HSV-2 to cell surface heparan sulfate proteoglycans, were formulated as topical vaginal gels (8, 9). However, clinical trials failed to demonstrate any protective benefit, possibly reflecting difficulties with adherence, low potency, particularly in the setting of semen, and unanticipated subclinical toxicities (10–12).

Alternative approaches include the development of more-specific inhibitors of viral entry and/or the targeting of other steps in the viral life cycle. However, these approaches are difficult, because HSV entry and dissemination are complex. For example, both serotypes may enter via direct fusion of the viral envelope with the cellular plasma membrane or by various endocytic mechanisms; the entry pathway may depend on the relative expression of viral coreceptors and access to various signaling pathways on different cell types (13–15). The mechanisms of viral assembly, egress, and cell-to-cell spread are also complex and not fully defined. Identification of molecules that contribute to more than one step in the viral life cycle and that are common for viral infection of multiple cell types may provide targets for the development of new preventative or therapeutic drugs.

Dynamin is such a candidate. Dynamin is a multidomain GTPase that controls multiple endocytic pathways and also plays a role in actin assembly and reorganization; thus, it may participate in viral entry, capsid formation, and transport (16). Prior studies found that dynasore, a cell-permeant small-molecule inhibitor of the GTPase activities of dynamin 1 and dynamin 2, blocked HSV-1 entry into human and murine keratinocytes, but not into murine hippocampal cells (17). No similar studies with human neuronal or primary genital tract cells or with HSV-2 have been

Received 9 March 2015 **Accepted** 10 April 2015

Accepted manuscript posted online 15 April 2015

Citation Mues MB, Cheshenko N, Wilson DW, Gunther-Cummins L, Herold BC. 2015. Dynasore disrupts trafficking of herpes simplex virus proteins. J Virol 89:6673–6684. doi:10.1128/JVI.00636-15.

Editor: R. M. Longnecker

Address correspondence to Betsy C. Herold, betsy.herold@einstein.yu.edu.

* Present address: Mascha B Mues, Praxis Hohenstaufenring, Cologne, Germany.

M.B.M. and N.C. contributed equally to this article.

doi:10.1128/JVI.00636-15

reported. We hypothesize that dynamin may also participate in other trafficking steps in the viral life cycle and therefore that dynasore may inhibit HSV infection postentry. Thus, focusing on human neuronal and female genital tract cells, we evaluated the impact of dynasore, added at the time of entry or postentry, on HSV-1 and HSV-2.

MATERIALS AND METHODS

Cells and viruses. SK-N-SH cells (a human neuroblastoma cell line; American Type Culture Collection [ATCC] HTB-11), CaSki cells (a human cervical epithelial cell line; ATCC CRM-CRL1550), and Vero cells (African green monkey kidney cells; ATCC CCL 81) were cultured in Dulbecco's modified Eagle medium (DMEM) supplemented with 10% fetal bovine serum. Cortical human fetal tissue was obtained as part of an ongoing research protocol approved by the Albert Einstein College of Medicine. Neuronal cell and astrocyte cultures were prepared as described previously (18–20). Primary genital tract cells were isolated from cervicovaginal lavage (CVL) cell pellets obtained from healthy women participating in studies of mucosal immunity after informed consent was obtained. The study was approved by the Albert Einstein College of Medicine IRB. The CVL fluid was subjected to low-speed centrifugation, and the cellular pellet was resuspended in serum-free medium, subjected to a second centrifugation step to remove mucus, and grown in keratinocyte medium (Life Technologies, Grand Island, NY). Vaginal epithelial cells (VK2/E6E7; ATCC CRL-2616) were also grown in keratinocyte medium.

HSV-2(G), HSV-1(KOS), HSV-2(333ZAG), expressing green fluorescent protein (GFP) under the control of a cytomegalovirus (CMV) promoter inserted into an intergenic region between UL3 and UL4 (a gift from P. Spear, Northwestern University), HSV-1(KVP26GFP), which contains a GFP-VP26 fusion protein (21), and HSV-1(F-GS2822), which encodes red fluorescent protein fused to the N terminus of VP26 (22), were prepared from infected Vero cell cultures, and viral stocks were stored at −80°C.

Reagents. Dynasore hydrate (catalog no. D7693; Sigma-Aldrich) and ML141 (catalog no. 4266; Tocris Bioscience) were reconstituted in dimethyl sulfoxide (DMSO) and serum-free medium (8 to 80 μM dynasore and 10 or 100 μM ML141; the final concentration of DMSO was 0.25% for 80 μM dynasore and 100 μM ML141). The control buffer was serum-free medium with 0.25% DMSO. Heparin (American Pharmaceutical Partners, Schaumburg, IL) was used at a final concentration of 100 μg/ml and nonoxynol-9 (Sigma) at a final concentration of 0.01%.

Primary antibodies and dilutions for Western blotting, proximity ligation assays, or confocal imaging were as follows: a mouse anti-VP16 monoclonal antibody (MAb) (sc-7545; dilution, 1:500; Santa Cruz Biotechnology, Santa Cruz, CA, USA), an anti-VP5 MAb (sc-56989; dilution, 1:200), an anti-gD MAb (sc-56988; dilution, 1:1,000), anti-glial fibrillary acidic protein (anti-GFAP) (antibody 3670; Cell Signaling, Danvers, MA), an anti-β-actin MAb (A-5441; dilution, 1:5,000; Sigma-Aldrich), an anti-histone H1 MAb (sc-8030; dilution, 1:250), an anti-golgin 97 MAb (sc-59820; dilution, 1:250), an anti-ICP0 MAb (sc-53070; dilution, 1:500), and a rabbit anti-dynamin antibody (sc-11362). The secondary antibodies for Western blotting were horseradish peroxidase-conjugated goat anti-mouse (catalog no. 170-5047; Bio-Rad) and goat anti-rabbit (catalog no. 170-5046; Bio-Rad) antibodies. The secondary antibodies for confocal microscopy were Alexa Fluor 488-, Alexa Fluor 555-, or Alexa Fluor 350-conjugated anti-mouse antibodies and Alexa Fluor 488- or Alexa Fluor 350-conjugated anti-rabbit antibodies (catalog no. A-11001, A-21422, A-11045, A-11008, and A-21068; Invitrogen Molecular Probes). All secondary antibodies were diluted 1:1,000.

Infectivity assays. For plaque assays, cells were first pretreated with drugs or a control buffer for 20 min at 37°C and then infected with HSV-1 or HSV-2 at the multiplicities of infection (MOI) indicated below. After 1 h of incubation at 37°C (referred to as the entry period), the cells were washed three times to remove unbound virus and drug and were overlaid with 0.5% methylcellulose. Plaques were counted 24 to 48 h later, after staining of the cells with Giemsa stain. In parallel studies, the cytotoxicities of the drugs were assessed using an MTS [3-(4,5-dimethylthiazol-2-yl)-5-(3-carboxymethoxyphenyl)-2-(4-sulfophenyl)-2H-tetrazolium] assay. Because virus does not plaque well on primary neuronal cells, the primary fetal astrocytes or neurons were infected as described above except that the overlay was fresh medium; culture supernatants were collected 24 h postinfection (p.i.), and viral progeny were quantified by determining the titers of the supernatants on Vero cells. In other studies, dynasore or ML141 was added at different times postentry, and the effect on infection was monitored either by a plaque assay or by harvesting cell lysates, preparing nuclear or cytosolic extracts, and performing Western blotting for viral gene expression as described previously (15, 23, 24). For examination of the purity of isolated cellular fractions, golgin 97 and histone H1 were included in the blots as markers of cytoplasmic and nuclear fractions, respectively.

To evaluate the impact of dynasore on other steps in the viral life cycle, single-step and multistep viral growth studies were performed. SK-N-SH cells were infected with HSV-2(G) (MOI, 5 PFU/cell) for 1 h at 37°C. Cells were first washed for 2 min with a low-pH citrate buffer (40 mM citric acid, 10 mM KCl, 135 mM NaCl [pH 3.0]) to inactivate extracellular virus, then washed three times with medium, and finally overlaid with 199V supplemented either with 0.25% DMSO or with dynasore (80 μM). The culture supernatants were harvested 4 h, 8 h, and 16 h p.i. and were stored at −80°C. The culture supernatants were diluted 1:10 with serum-free medium (to dilute any residual dynasore to noninhibitory concentrations of 8 μM) and were plated on Vero cells to measure infectious virus. For multistep growth assays, the cells were infected with HSV-2(G) at an MOI of 0.02 PFU/cell for 1 h; the inoculum was removed; and the cells were overlaid with fresh medium. Dynasore (or a control DMSO buffer) was added to the cultures 6 h p.i., and culture supernatants were harvested 14, 24, 36, or 48 h p.i., diluted 1:10 as described above, and assayed for infectious progeny by plating on Vero cells.

Binding and entry assays. Cells were first treated with dynasore or a control buffer for 20 min, then transferred to 4°C, and exposed to virus (MOI, 0.1 and 1 PFU/cell) for 4 h to allow binding. Unbound virus was removed by washing, and the cell-bound virus was analyzed by preparing Western blots of cell lysates and probing with anti-gD MAb 1103 (Virusys, Sykesville, MD) (25). To examine the effects of dynasore on entry, cells were infected with virus (MOI, 1 PFU/cell) in the presence or absence of drug, and nuclear extracts were prepared 1 h p.i. and were analyzed by preparing Western blots for VP16, a tegument protein, as described previously (23).

Alternatively, to monitor viral entry, cells were grown on glass coverslips in 12-well plates, synchronously infected with HSV-1(KVP26GFP) in the presence or absence of dynasore, and fixed with 4% paraformaldehyde (Electron Microscopy, Hatfield, PA) 1 h p.i. for confocal microscopy as described previously; nuclei were stained with 4′,6-diamidino-2-phenylindole (DAPI) (26). In other experiments, dynasore or a control buffer was added 3 or 7 h p.i., and after an additional 1-h incubation, the cells were fixed with 4% paraformaldehyde and were stained for microtubules with an anti-α-tubulin MAb (clone 236-1050; Life Technologies). Cells were visualized using a Zeiss Live DuoScan confocal microscope fitted with a 100× (numerical aperture, 1.4) oil objective.

Transferrin assay. Cells were seeded at 500,000/well on glass coverslips in 12-well plates for 48 h. The medium was removed after 1 day, and the cells were incubated overnight in supplement-free medium to remove any residual transferrin. On the day of the experiment, the cells were pretreated with 500 μl/well of 20 or 60 μM dynasore or a control DMSO buffer for 15 min. The cells were prechilled on ice for another 15 min and were then exposed to 25 μg/ml of Alexa 555-conjugated transferrin (Molecular Probes) for 1 h at 4°C. The cells were washed once with ice-cold phosphate-buffered saline (PBS) and were then shifted to 37°C for 30 min. Transferrin uptake was terminated by washing the cells three times with ice-cold PBS. The cells were stained with the lipophilic tracer DiO (dilu-

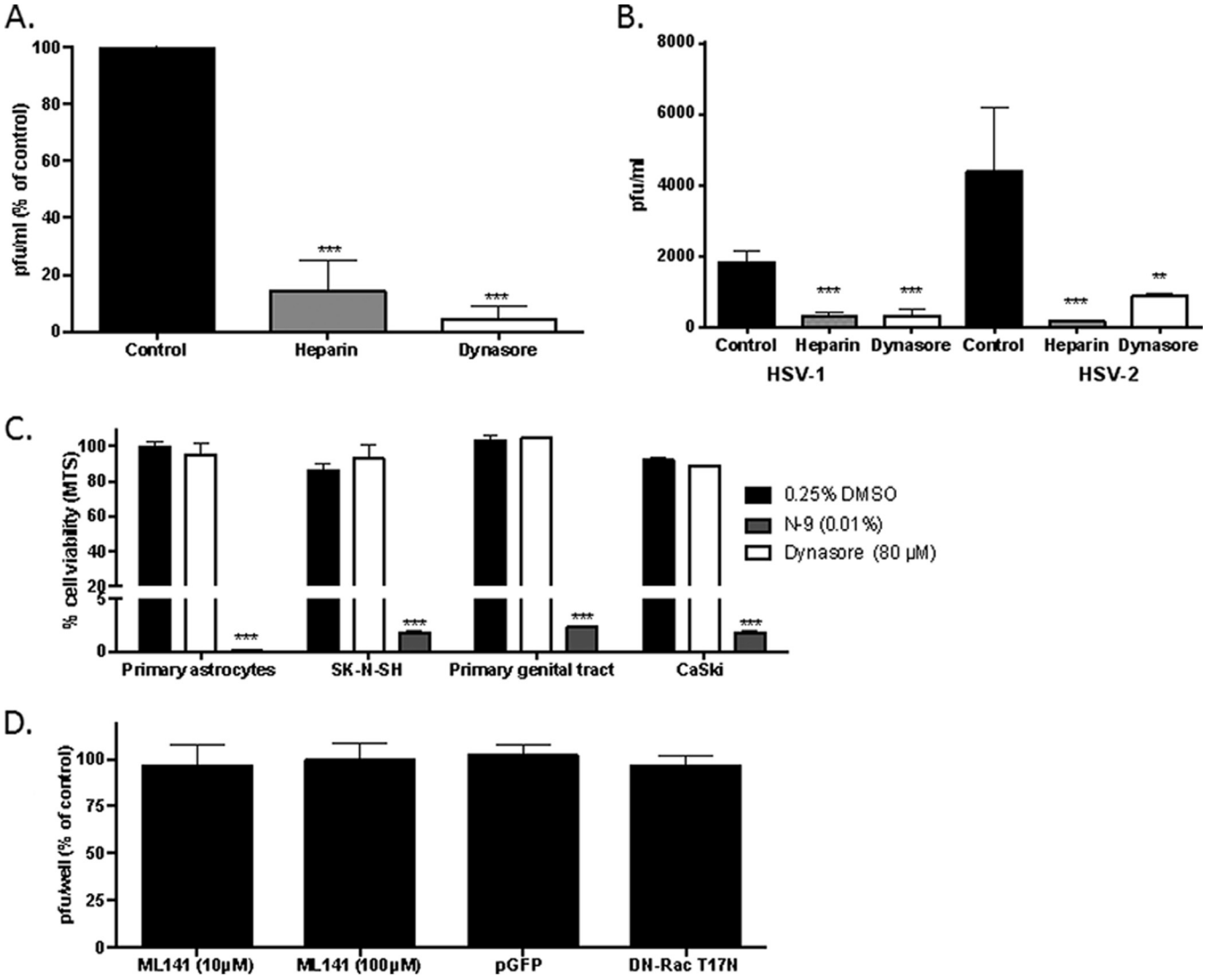

FIG 1 Dynasore inhibits HSV infection. (A) SK-N-SH (human neuroblastoma) cells were first incubated with dynasore (80 μM), heparin (100 μg/ml), or a control DMSO buffer and then infected with HSV-2(G) for 1 h. The cells were washed and were overlaid with fresh medium, and plaques were counted at 48 h. (B) Primary human astrocytes were infected with HSV-1(KOS) or HSV-2(G) (MOI, 5 PFU/cell) in the presence of dynasore, heparin, or a control DMSO buffer, and infectious progeny were quantified by plating serial dilutions of the supernatants on Vero cells. (C) Cells were treated with 80 μM dynasore, 0.01% nonoxynol-9 (N-9) as a positive control, or 0.25% DMSO as a negative control for 48 h, and toxicity was assessed by an MTS assay. Results are presented as means + standard errors of the means from three independent experiments, each conducted in duplicate; the asterisks indicate differences from the control as determined by an unpaired *t* test or analysis of variance (**, $P < 0.01$; ***, $P < 0.001$). (D) SK-N-SH cells were first treated with 10 or 100 μM ML141 or with a 0.25% DMSO control buffer and then infected with HSV-2(G), and plaques were counted after 48 h of incubation. Alternatively, the cells were transfected with a plasmid expressing the dominant negative form of Rac 1 (DN-RacT17N) or a control GFP-expressing plasmid (pmaxGFP) and were infected with HSV-2(G) 24 h later, and plaques were quantified 48 h p.i. Results are presented as means + standard errors of the means from two experiments conducted in duplicate.

tion, 1:200; Molecular Probes), washed three times with PBS, and fixed with 4% paraformaldehyde for 30 min at room temperature. The cells were then incubated overnight in a blocking solution containing 3% bovine serum albumin (BSA), and the nuclei were stained for 10 min with DAPI (1:2,000), washed, mounted on glass slides using ProLong Gold antifade reagent (Invitrogen), and visualized using a Zeiss Live DuoScan confocal microscope fitted with a 64× (numerical aperture, 1.4) oil objective. Z-sections were captured in an optical slice of 0.44 μm. Extended-focus images were generated using Volocity confocal software (version 6.3; Improvision, Lexington, MA).

Coculture assay. Primary human neuronal cells were infected with HSV-1(KVP26GFP) (10 PFU/cell) for 1 h at 37°C; then unbound virus was washed off, and the cells were trypsinized and cocultured on a layer of untreated CaSki cells (~90% confluence) on glass coverslips at ratios of ~1:4 and 1:10 (infected neuronal cells to uninfected CaSki cells) in a medium containing pooled human immunoglobulin G (IgG) (1990 medium; Sigma) (1990). At 5 h postinfection, dynasore (80 μM in 0.25% DMSO) or a control medium (containing 0.25% DMSO) was added to these cocultures. At 18 h p.i., the cells were fixed with 4% paraformaldehyde and were stained first with a primary antibody against GFAP (antibody 3670; Cell Signaling, Danvers, MA) and then with an Alexa Fluor 647-conjugated secondary antibody (catalog no. A21463; Invitrogen) and DAPI for analysis by confocal microscopy. Images were obtained as Z-sections in an optical slice of 0.6 to 0.8 μm, and maximal Z-projections were analyzed in order to compare viral spread.

Transfections. Cells were transfected with plasmids expressing dominant negative forms of dynamin 1 (K44Adnm1), dynamin 2 (K44Adnm2) (Addgene, Cambridge, MA), or Rac1 (pDN-RacT17N) (a

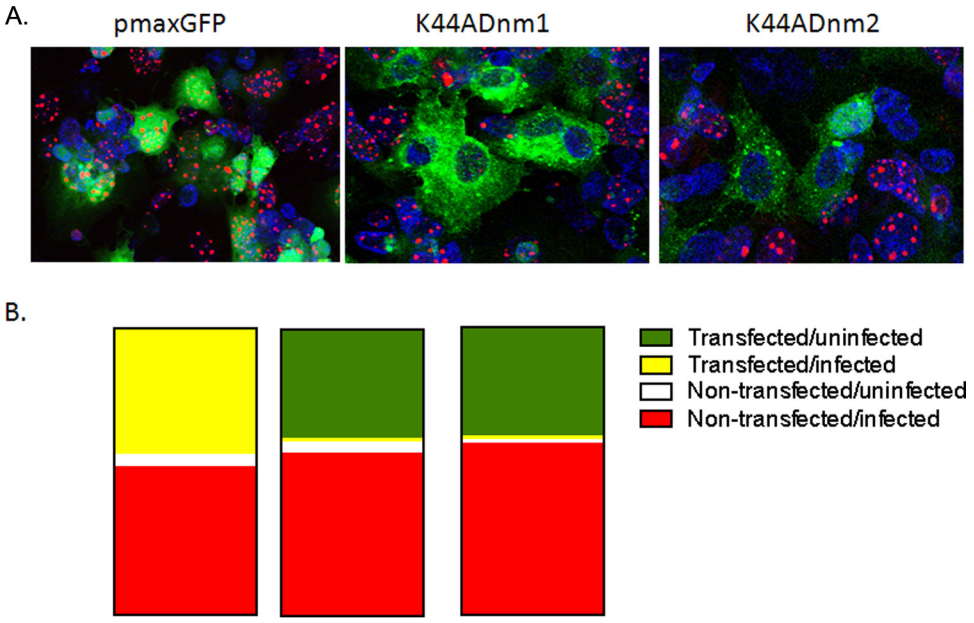

FIG 2 Transfection of cells with dominant negative dynamin inhibits HSV infection of neuronal cells. SK-N-SH cells were transfected with a plasmid expressing the dominant negative form of dynamin 1 (K44Adnm1) or dynamin 2 (K44Adnm2) or with a control GFP-expressing plasmid (pmaxGFP). Twenty-four hours later, the cells were infected with HSV-1(F-GS2822) (MOI, 10), which encodes the red fluorescent protein fused to the N terminus of VP26. Cells were fixed 16 h p.i., and nuclei were stained with DAPI (blue). (A) Representative images from two independent experiments. (B) Proportions of transfected, uninfected (green), transfected, infected (yellow), nontransfected, uninfected (white), and nontransfected, infected (red) cells, quantified after a review of 5 independent fields (total of 100 cells). (Left) pmaxGFP; (center) K44Adnm1; (right) K44Adnm2.

gift from Jonathan Backer, Department of Pharmacology, Albert Einstein College of Medicine) or with a control GFP-expressing plasmid (pmaxGFP) by using Effectene transfection reagent (Qiagen, Germantown, MD).

Electron microscopy (EM) imaging. SK-N-SH cells were grown in 60-mm dishes and were infected with HSV-2(G) at an MOI of 5 PFU/cell for 1 h at 37°C. Unbound virus was removed by washing, and the cells were overlaid with a control medium containing 0.25% DMSO or a medium containing 80 μM dynasore. At 16 h p.i., the cell monolayers were fixed with 2.5% glutaraldehyde in 0.1 M sodium cacodylate buffer, postfixed with 1% osmium tetroxide followed by 2% uranyl acetate, and dehydrated through a graded ethanol series; then the cells were lifted from the monolayer with propylene oxide and were embedded as a loose pellet in LX-112 resin (Ladd Research Industries, Burlington, VT) in Eppendorf tubes. Ultrathin sections were cut on a Reichert Ultracut UCT instrument, stained with uranyl acetate followed by lead citrate, and viewed on a JEOL 1200EX transmission electron microscope at 80 kV.

Capsid purification. SK-N-SH cells were infected at an MOI of 10 PFU/cell, and 6 h p.i., dynasore or 0.25% of DMSO in serum-free medium was added. The cells were harvested 16 h p.i., subjected to low-speed centrifugation for 10 min, and washed once in Dulbecco's phosphate-buffered saline (catalog no. 21-031-CV; Corning cellgro; Mediatech, Manassas, VA). The cell pellet was resuspended in an equal volume of 2× lysis buffer containing 1 M NaCl, 20 mM Tris (pH 7.6), 2 mM EDTA, 2% Triton X-100, and one complete protease inhibitor cocktail tablet (Boehringer Mannheim) per 25 ml of lysis buffer. Cells were lysed by freeze-thawing, and cytoplasmic and nuclear fractions were separated by centrifugation at 3,000 rpm for 15 min. The nuclear pellet was dissolved in lysis buffer and was purified of cytoplasmic contamination by centrifugation through a 30% (wt/vol) sucrose cushion. Capsids from cytoplasmic and nuclear fractions were purified by two centrifugation steps. In the first step, capsids were centrifuged through a 35% (wt/vol) sucrose cushion prepared in a buffer containing 500 mM NaCl, 20 mM Tris (pH 7.6), and 1 mM EDTA (TNE). The capsid pellet was then resuspended in TNE, and capsids were purified on 20- to 50% (wt/vol) sucrose gradients centrifuged at 24,000 rpm for 60 min. Capsids were visualized as light-scattering bands and were collected by aspiration into a syringe. Capsids were analyzed by SDS-PAGE and silver staining.

Proximity ligation assay. SK-N-SH cells (~10^5/well) were seeded on microscope glass cover slides in a 24-well plate (Fisher Scientific) and were either infected with purified viruses (MOI, 5 to 10 PFU/cell) or mock infected for the times indicated in the legend to Fig. 7 at 37°C. Dynasore was added 7 h p.i., and 1 h later, the cells were fixed with cold 4% paraformaldehyde. A blocking solution from a Duolink In Situ kit was used to prevent nonspecific interactions. Cells were incubated with rabbit anti-dynamin and mouse anti-VP5 diluted 1:100 in 3% BSA in PBS for 1 h at room temperature. Proximity ligation assays were performed with the anti-mouse Minus and anti-rabbit Plus Duolink In Situ PLA probes (catalog no. DUO92004 and DUO092002, respectively; Sigma-Aldrich) according to the manufacturer's protocol. Fluorescence signals were detected using a Zeiss Live DuoScan confocal microscope fitted with a 64× (numerical aperture, 1.4) oil objective. Z-sections were captured in an optical slice of 0.44 μm. Extended-focus images were generated using Volocity confocal software (version 5; Improvision, Lexington, MA).

Statistical analysis. All experiments were conducted at least in duplicate, and at least two independent experiments were performed. GraphPad Prism (version 6; GraphPad Software) was used for statistical analysis of results using Student's *t* test. Differences were considered significant at a P value of <0.05.

RESULTS

Dynamin inhibitors block HSV infection. SK-N-SH (human neuroblastoma) cells were first incubated with dynasore, heparin (an inhibitor of HSV binding [27]), or a control buffer (0.25% DMSO) and then infected with HSV-2(G) for 1 h. The cells were washed and were overlaid with fresh medium, and plaques were

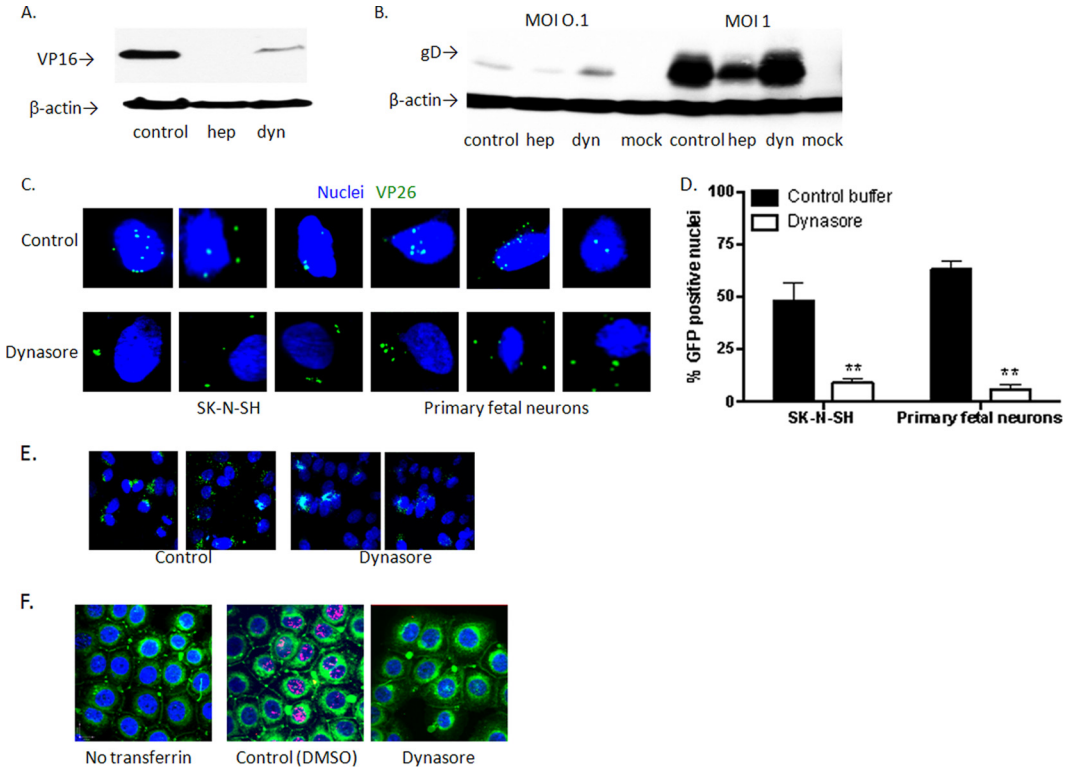

FIG 3 Dynasore blocks HSV-1 and HSV-2 entry into human neuronal cells. (A) SK-N-SH cells were pretreated with dynasore, heparin, or a control buffer and were then exposed to the virus at 37°C for 1 h. Western blots of nuclear extracts were probed with antibodies to VP16, a viral tegument protein that is transported to the nucleus within the first hour of viral entry, and β-actin (as a control). (B) SK-N-SH cells were pretreated with the drugs for 1 h at 37°C, then cooled to 4°C, a temperature permissive for viral binding but not entry, and finally exposed to HSV-2 at an MOI of 0.1 or 1 PFU/cell for 4 h. The cells were then washed, and cell lysates were prepared and were analyzed for the presence of bound viral particles by immunoblotting for the viral envelope glycoprotein D (gD). (C) Dynasore- or control buffer-treated SK-N-SH or primary fetal neuronal cells were synchronously infected with HSV-1(KVP26GFP) and were then fixed and stained with DAPI (blue). Confocal images were obtained 1 h after incubation at 37°C. Images of representative cells are shown. (D) GFP-positive nuclei were counted in five independent fields (100 cells), and percentages are shown. Asterisks indicate *P* values of <0.01 (by *t* test). (E) SK-N-SH cells were infected with HSV-1(KVP26GFP) and, after 1 h, were washed with a low-pH citrate buffer to inactivate extracellular virus. Then dynasore or a control buffer was added for an additional 1 h of incubation. Cells were then fixed and stained with DAPI (blue), and extended-focus confocal images were obtained. Two representative fields are shown for each condition. (F) Vaginal epithelial cells (VK2/E6/E7) were pretreated with 60 μM dynasore or a control buffer and were subsequently exposed to Alexa Fluor 555-conjugated transferrin (red) or a buffer (no transferrin) as described in Materials and Methods. Representative extended-focus images are shown. The plasma membranes were stained green with the lipophilic tracer DiO; cells were fixed; and nuclei were stained blue with DAPI. Images and blots are representative of at least two independent experiments.

counted at 48 h. Dynasore and heparin significantly reduced the number of viral plaques formed by 80 to 90% (Fig. 1A). To further explore the impact of dynasore on HSV infection of neuronal cells, experiments were performed using primary human glial cells. Because virus does not plaque well on these cells, culture supernatants of cells infected with HSV-1(KOS) or HSV-2(G) at an MOI of 5 were harvested 24 h p.i., and infectious progeny were quantified by plating serial dilutions of the supernatants on Vero cells. Both dynasore and heparin significantly reduced the number of viral progeny from that for controls (Fig. 1B). The concentration of dynasore used (80 μM) was based on prior studies (28–30) and was not cytotoxic by an MTS assay; nonoxynol-9 was included in the MTS assay as a positive toxicity control (Fig. 1C).

To determine the specificity of the effects of dynamin compared to other GTPase proteins on HSV infection, SK-N-SH cells were either treated with ML141, an allosteric inhibitor of Cdc42 GTPase, or transfected 24 h prior to infection with a plasmid expressing the dominant negative form of Rac1 (pDN-RacT17N) or a control plasmid, pmaxGFP. Based on microscopy, the transfection efficiency was 40 to 45% for both plasmids (not shown). Neither treatment with ML141 nor transfection with the dominant negative form of Rac1 had any impact on HSV infection (Fig. 1D).

To further assess the impact of dynasore on HSV infection, SK-N-SH cells were transfected with a plasmid expressing the dominant negative form of dynamin 1 (K44Adnm1) or dynamin 2 (K44Adnm2) or with a control GFP-expressing plasmid (pmaxGFP), and 24 h later, the cells were infected with HSV-1(F-GS2822) (MOI, 10), which encodes the red fluorescent protein fused to the N terminus of VP26. Cells were fixed and stained 16 h p.i., and 5 independent fields (total of 100 cells) were counted. There was no difference in transfection efficiency; ~50% of the cells stained green in each field (Fig. 2A and B). Infected cells (red marker labeling VP26) were detected in both nontransfected and transfected (green; merge, yellow) cells in the pmaxGFP cultures but were observed almost exclusively in nontransfected cells in the K44Adnm1 or K44Adnm2 cultures. Together, these observations indicate that dynamin plays a role in HSV infection but do not delineate which steps in the viral life cycle are impeded.

Dynasore blocks HSV-1 and HSV-2 entry and nuclear transport in human neuronal cells. To determine whether the inhibi-

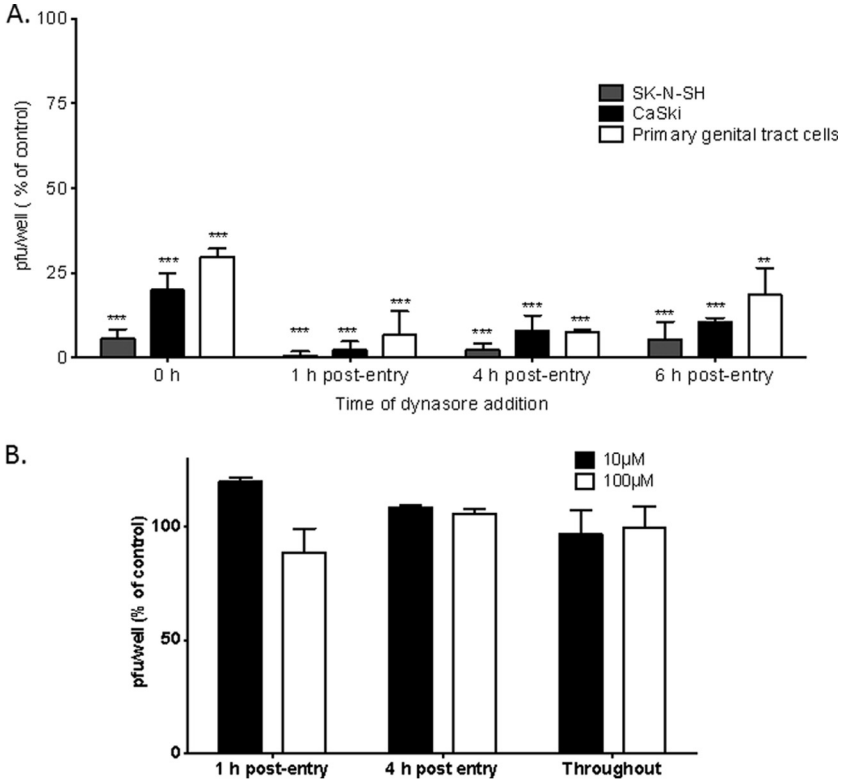

FIG 4 Dynasore inhibits HSV infection postentry. (A) SK-N-SH, CaSki, or primary human female genital tract cells isolated from cervicovaginal lavage fluid were first infected with HSV-2(G) for 1 h at 37°C, then washed, and finally overlaid with fresh medium. Dynasore was added either during the 1-h entry period, followed by washing of the cells (0 h postentry), or 1, 4, or 6 h postentry. Plaques were counted 24 h (for SK-N-SH cells) or 48 h (for CaSki and primary genital tract cells) p.i. (B) SK-N-SH cells were infected with HSV-2(G), and ML141 (10 or 100 μM) either was added 1 or 4 h postentry or was maintained in the cultures throughout the infection. Results are presented as the percentages of reduction in PFU from the level for cells treated with a control buffer (0.25% DMSO in serum-free medium). Asterisks indicate significance ($P < 0.001$) by *t* test.

tory effect observed reflected a block in entry, SK-N-SH cells were pretreated with dynasore, heparin, or a control buffer and were then exposed to virus at 37°C for 1 h. Dynasore reduced the level of HSV-2 entry as assessed by Western blotting of nuclear extracts for VP16, a viral tegument protein that is transported to the nucleus within the first hour of viral entry (Fig. 3A). To determine if viral binding was impacted, the cells were pretreated with the drugs for 1 h at 37°C, followed by cooling to 4°C, a temperature permissive for viral binding but not entry, and were exposed to HSV-2 at an MOI of 0.1 or 1 PFU/cell for 4 h. The cells were then washed, and cell lysates were prepared and analyzed for the presence of bound viral particles by immunoblotting for the viral envelope glycoprotein D (gD). Heparin, but not dynasore, inhibited viral binding (Fig. 3B).

Inhibition of viral entry was also observed when SK-N-SH or primary fetal neuronal cells were treated with dynasore and synchronously infected with HSV-1(KVP26GFP); confocal images were obtained 1 h after the temperature shift to 37°C. Viral capsids (VP26) (green) colocalized with nuclei were readily detected in control cells but not in dynasore-treated cells (Fig. 3C). The numbers of GFP^+ nuclei were significantly reduced in dynasore-treated cells ($P < 0.01$); five independent fields (total of 100 cells) were counted (Fig. 3D). In contrast, if the addition of dynasore was delayed, and the drug was added immediately following treatment with a low-pH citrate buffer after the 1-h entry period, there was no difference in the number of intracellular capsids detected by microscopy 1 h later (Fig. 3E). Dynasore blocked transferrin uptake in all of the cell types; representative extended-focus confocal images of transferrin uptake in vaginal epithelial cells (VK2/E6E7) are shown on Fig. 3F. Together, these findings indicate that dynasore inhibits HSV-1 and HSV-2 infection at least in part by impeding entry as defined by the nuclear transport of tegument proteins and capsids in the first hour following exposure to the virus.

Dynasore also inhibits HSV infection postentry. To assess whether dynasore also acted postentry, the time of addition of the drug was varied, and the effects on human neuronal and nonneuronal cells were explored. SK-N-SH cells, human cervical epithelial (CaSki) cells, or primary human female genital tract cells isolated from cervicovaginal lavage fluid were infected with HSV-2 for 1 h at 37°C, washed, and overlaid with fresh medium. Dynasore was added either during the 1-h entry period, followed by washing of the cells, or 1, 4, or 6 h postentry. Plaques were counted 24 h (for SK-N-SH cells) or 48 h (for CaSki and primary genital tract cells) p.i. Dynasore significantly reduced viral plaque formation when added at the time of entry but was highly potent when added 1, 4, or 6 h postentry (Fig. 4A). In contrast, ML141 had no impact on viral plaque formation when added postentry or maintained throughout the experiment (Fig. 4B).

To further differentiate the effects of dynasore on viral entry or postentry events, additional kinetic studies were conducted with increasing doses of dynasore. Primary fetal neuronal cells were

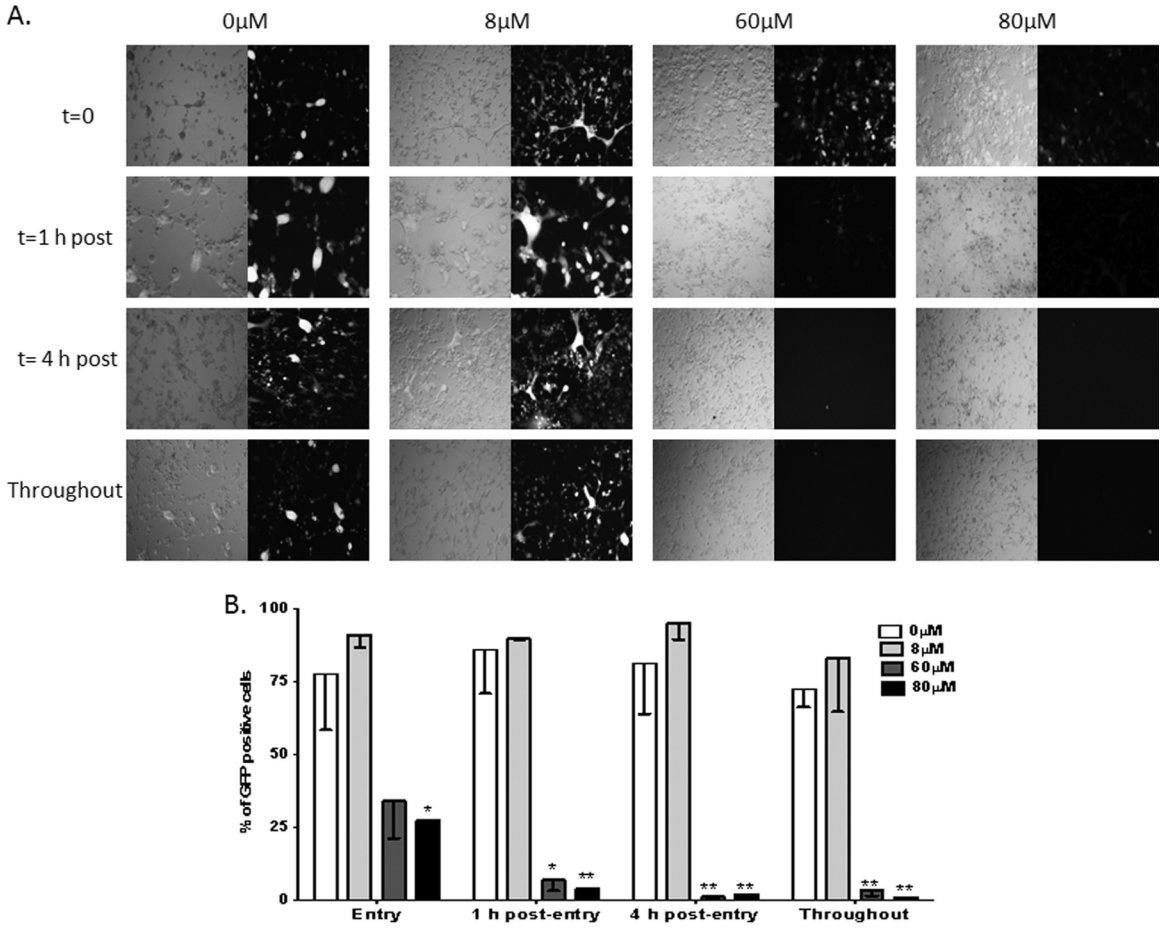

FIG 5 Dynasore has potent postentry effects on HSV infection of primary fetal neuronal cells. Fetal neuronal cells were infected with the GFP-expressing virus HSV-2(333ZAG) (MOI, 0.5 PFU/cell). After 1 h of incubation, the cells were treated with a citrate buffer to inactivate any virus that had not yet penetrated them, washed, and overlaid with fresh medium. Dynasore or a 0.25% DMSO control buffer was either added once, at the time of infection ($t = 0$), immediately after citrate treatment ($t = 1$), or 4 h after citrate treatment ($t = 4$), or was added both at the time of infection and after citrate treatment (throughout). (A) Representative fluorescence microscopy images of live cells 48 h postinfection. (B) Percentages of cells that were infected (GFP positive), quantified after review of several independent fields (500 to 600 cells).

infected with HSV-2(333ZAG) (MOI, 0.5 PFU/cell), which expresses GFP under the control of a CMV promoter. After 1 h of incubation, the cells were treated with a citrate buffer to inactivate any virus that had not yet penetrated them, washed, and overlaid with fresh medium. Dynasore or a 0.25% DMSO control buffer was added either at the time of infection, immediately after citrate treatment, 4 h after citrate treatment, or both at the time of infection and post-citrate treatment (throughout). Live cells were imaged by fluorescence microscopy 48 h postinfection (Fig. 5A). Concentrations of 60 or 80 μM dynasore almost completely blocked viral infection when added postentry, whereas 8 μM had no inhibitory effect. If the drug was added only at the time of entry, partial inhibition was observed, which was statistically significant only at 80 μM (Fig. 5B). These findings further support a potent postentry effect of dynasore.

Dynasore prevents the transport of viral proteins from the nucleus to the cytoplasm. The postentry effects of dynasore suggest that dynamin may be involved in the trafficking of viral components needed for capsid and viral particle assembly. To explore this possibility, cells were infected with HSV-2(G) (MOI, 1 PFU/cell), and a control buffer or dynasore was added 0, 4, and 8 h p.i. Nuclear and cytoplasmic extracts were prepared 24 h p.i. and were probed for VP5 and ICP0. Reductions in VP5 and ICP0 levels were detected in the cytoplasm and nucleus when dynasore was added at the time of viral entry (0 h p.i.) (Fig. 6A), in agreement with the effects of dynasore on entry (Fig. 3, 4, and 5). However, when dynasore was added 4 or 8 h p.i., the viral proteins were retained almost exclusively in the nuclear fraction (identified by probing with anti-histone-associated protein 1 [anti-H1]), not in the cytoplasm (identified by probing with anti-golgin), indicating that dynasore prevents the accumulation of VP5 and ICP0 in the cytoplasm (Fig. 6A). Similar results were obtained when blots were probed for ICP4 or VP16; these proteins also were retained almost exclusively in the nuclear fraction (not shown).

The notion that viral proteins were trapped in the nucleus was also suggested by confocal microscopy studies using the HSV-1 strain containing a VP26-GFP fusion protein. Dynasore was added 3 h or 7 h p.i. One hour later, the cells were fixed and were stained for microtubules (red) and nuclei (blue). There was little or no difference between confocal images for control and dynasore-treated cells when dynasore was added 3 h p.i. and imaged 1 h later (4 h p.i.); the majority of VP26-GFP was detected in asso-

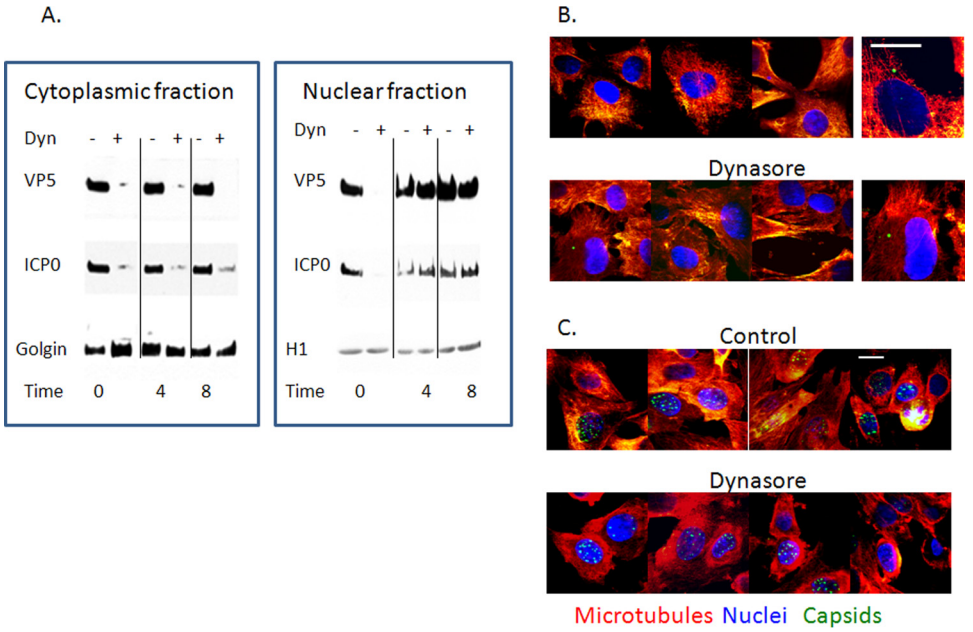

FIG 6 Dynasore prevents the transport of viral proteins from the nucleus to the cytoplasm. (A) SK-N-SH cells were infected with HSV-2(G) (MOI, 1 PFU/cell), and dynasore or a control buffer was added 0, 4, or 8 h p.i. Cytoplasmic and nuclear fractions were isolated 24 h p.i. Immunoblots were prepared and were probed for VP5, ICP0, golgin, and histone-associated protein 1 (H1). No H1 was detected in cytoplasmic fractions and no golgin in nuclear fractions. Immunoblots are representative of 3 independent experiments. (B and C) SK-N-SH cells were infected with HSV-1(KVP26GFP) (MOI, 10 PFU/cell). Dynasore or a control buffer was added 3 h p.i. (B) or 7 h p.i. (C). The cells were subsequently fixed and were stained 1 h later for microtubules (red) and nuclei (blue). Bars, 10 μM. Images are representative of two independent experiments.

ciation with microtubules (Fig. 6B). In contrast, when dynasore was added at 7 h and images were obtained 1 h later, VP26-GFP appeared to be trapped in the nucleus, whereas in control cells, VP26-GFP was readily detected both inside and outside the nucleus (Fig. 6C). The notion that dynasore interferes with the transport of viral proteins out of the nucleus was further substantiated by a proximity ligation assay with antibodies to dynamin and VP5. Dynasore was again added 7 h p.i., and cells were stained 1 h later. Colocalization of dynamin and VP5 (red) was observed in both control and dynasore-treated cells 1 h after the addition of dynasore (8 h p.i.); however, VP5-dynasore colocalization was confined primarily to the nucleus (stained blue with DAPI; merge, purple) in dynasore-treated cells but was readily detected outside the nucleus in control cells (Fig. 7).

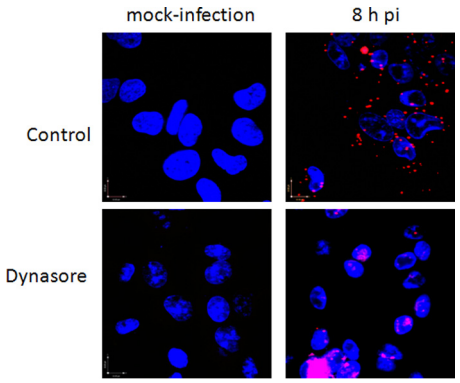

FIG 7 Dynamin interacts with the HSV major capsid protein. SK-N-SH cells were infected with HSV-2(G), and dynasore or a control buffer was added 7 h p.i. Cells were fixed 1 h later, probed with monoclonal mouse antibodies to the major capsid protein, VP5, and with a rabbit antiserum to dynamin, and assessed by a proximity ligation assay. Representative fields (magnification, ×64) from two independent experiments are shown.

Viral capsids are restricted to the nucleus in dynasore-treated cells. To evaluate whether dynasore prevents capsid transport, electron microscopy studies were also performed. SK-N-SH cells were infected with virus; dynasore (or a control buffer) was added 1 h p.i.; and images were obtained 16 to 18 h p.i. Viral capsids were easily detected in the cytoplasm and intercellular spaces in control cells (Fig. 8A and B) but were observed only infrequently in dynasore-treated cells, where they were restricted to the nucleus (Fig. 8C and D). In addition, when dynasore was added 6 h p.i., and capsids were purified from cytoplasmic and nuclear fractions 18 h p.i. and were analyzed by Western blotting, VP5 was readily detected in the nuclear fractions of both control and dynasore-treated cells, but VP5 levels were markedly reduced in capsids isolated from the cytoplasm (Fig. 8E and F). No difference in total VP5 levels between unfractionated dynasore- or control buffer-treated lysates was detected by Western blotting (Fig. 8G).

Dynasore prevents cell-to-cell spread. The observations that dynasore inhibits capsid and capsid protein transport to the nucleus at early time points and transport out of the nucleus at later times p.i. indicate that it should also block cell-to-cell spread of the virus. To address this, additional studies were performed focusing on the spread of the virus from primary human neuronal cells to epithelial cells. Primary fetal neuronal cells (donors) were infected with a GFP-capsid-labeled virus for 1 h, washed, and then cocultured at a ratio of 1:4 or 1:10 with CaSki cells (receivers) in the presence of human antiserum. Dynasore or a control buffer was added to the medium 5 h after coculturing. The cells were fixed 18

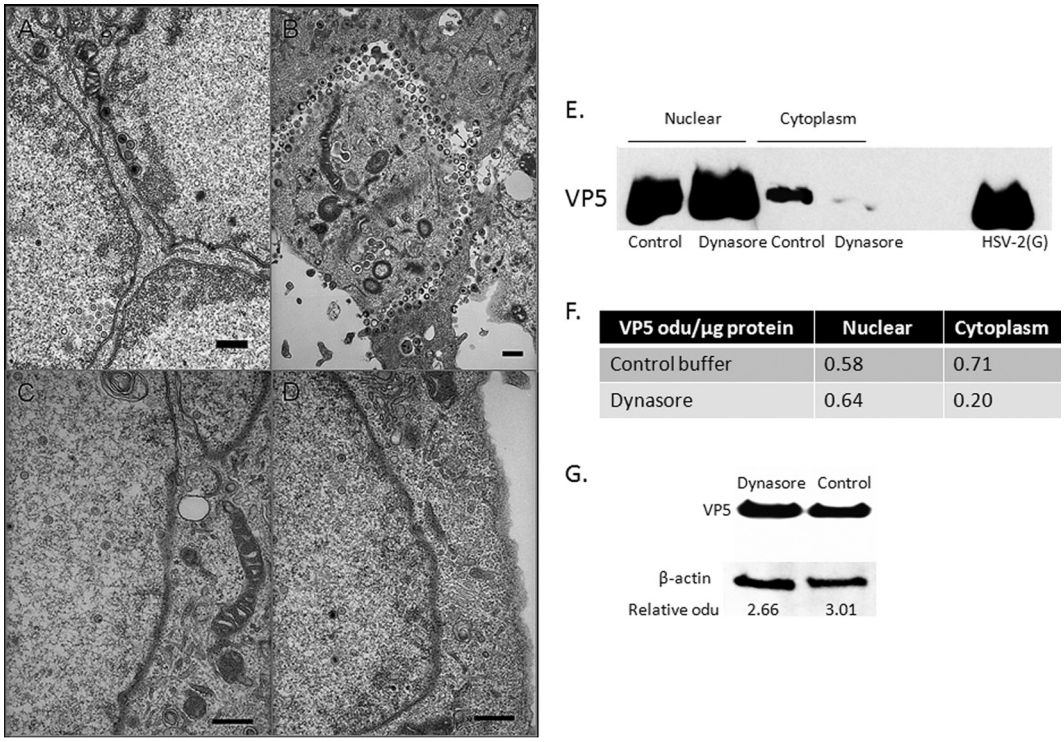

FIG 8 Viral capsids are restricted to the nucleus in dynasore-treated cells. (A to D) SK-N-SH cells were infected with HSV-2(G) (MOI, 5 PFU/cell) for 1 h at 37°C. After unbound virus was washed off, the cells were overlaid with either a control medium containing 0.25% DMSO or a medium containing 80 μM dynasore. At 16 h p.i., cells were fixed and were prepared for electron microscopy. Representative images from control (magnification, ×10,000) (A and B) and dynasore-treated (magnification, ×20,000) (C and D) cells from two independent experiments are shown. Bars, 500 nm. (E) SK-N-SH cells were infected at an MOI of 10 PFU/cell, and 6 h p.i., dynasore or 0.25% DMSO in serum-free medium was added. The cells were harvested 18 h p.i.; cytoplasmic and nuclear fractions were prepared; and capsids were purified on 20- to 50% (wt/vol) sucrose gradients. The capsids were analyzed by Western blotting and were probed with an antibody to VP5. Purified HSV-2(G) was included as a positive control. (F) Blots were scanned, and relative optical density units (odu) normalized for total protein per lane are shown. Results are representative of 3 independent experiments. (G) Unfractionated infected SK-N-SH cell pellets were analyzed in parallel for VP5; representative results are shown. Blots were scanned, and VP5 odu relative to β-actin odu are shown below each lane.

h p.i, stained with a neuronal cell marker (GFAP) (red) and with DAPI (nuclei) (blue), and imaged by confocal microscopy. Virus was restricted to the neuronal cells (red) in dynasore-treated cultures but was detected primarily in nonneuronal cells in the control plates. Dynasore reduced the number of GFP-positive receivers (CaSki cells) per donor (neuronal cell) from 4.36 ± 1.52 in control buffer-treated cultures to 0.31 ± 0.31 in dynasore-treated cultures (200 cells were counted in two independent experiments) (Fig. 9A). Moreover, single and multistep growth studies also indicated that the addition of dynasore postentry prevented viral dissemination; results for SK-N-SH cells are shown (Fig. 9B and C), and similar results were obtained with primary genital tract cells.

DISCUSSION

In agreement with prior studies with HSV-1 and other viruses, including Chikungunya virus (31), Japanese encephalitis virus (32), reoviruses (33), Ebola virus (34), and HIV (with HaCaT cells but not primary CD4 T cells) (29, 35, 36), dynasore inhibited the entry of HSV-1 and HSV-2 into human neuronal (SK-N-SH and fetal primary) and genital tract (CaSki and primary) cells. Entry was defined here as the successful transport of tegument (VP16) or capsid (VP26-GFP) proteins to the nuclear pore; thus, the inhibitory activity may reflect interference with one of several entry mechanisms, such as endocytosis or macropinocytosis and/or a block in capsid transport along the microtubular network. Dynasore was previously shown to inhibit HSV-1 entry into HaCaT cells and primary keratinocytes, but not into murine hippocampal neurons (17). However, we found that dynasore reduced entry into human neuroblastoma (SK-N-SH) cells and reduced viral yields when added during the first hour of infection of primary human fetal neuronal cells (Fig. 1B). Another recent study found that dynasore also decreased the expression of HSV-1 immediate early genes in Vero (monkey kidney epithelial), HeLa (human epithelial), HEp-2 (human epithelial), and PtK_2 (rat kangaroo epithelial kidney) cells (37). However, transfection of the cells with a dominant negative form of dynamin had little effect. In contrast, we found that transfection of human neuronal cells with dominant negative forms of dynamin reduced viral entry as measured by the transport of VP26 to the nucleus (Fig. 2). The differences between the observations of the current study and those of the previous studies likely reflect the different species, cell types, and/or viral strains.

While the studies confirm prior work indicating a role for dynamin in HSV entry, the novel observation is that dynasore exhibited potent inhibitory effects when added at later time points (4 to 8 h p.i.) (Fig. 4 to 8) and impeded the transport of capsid proteins from the nucleus to the cytoplasm, resulting in a decrease in the number of capsids. The postentry effects were specific for dy-

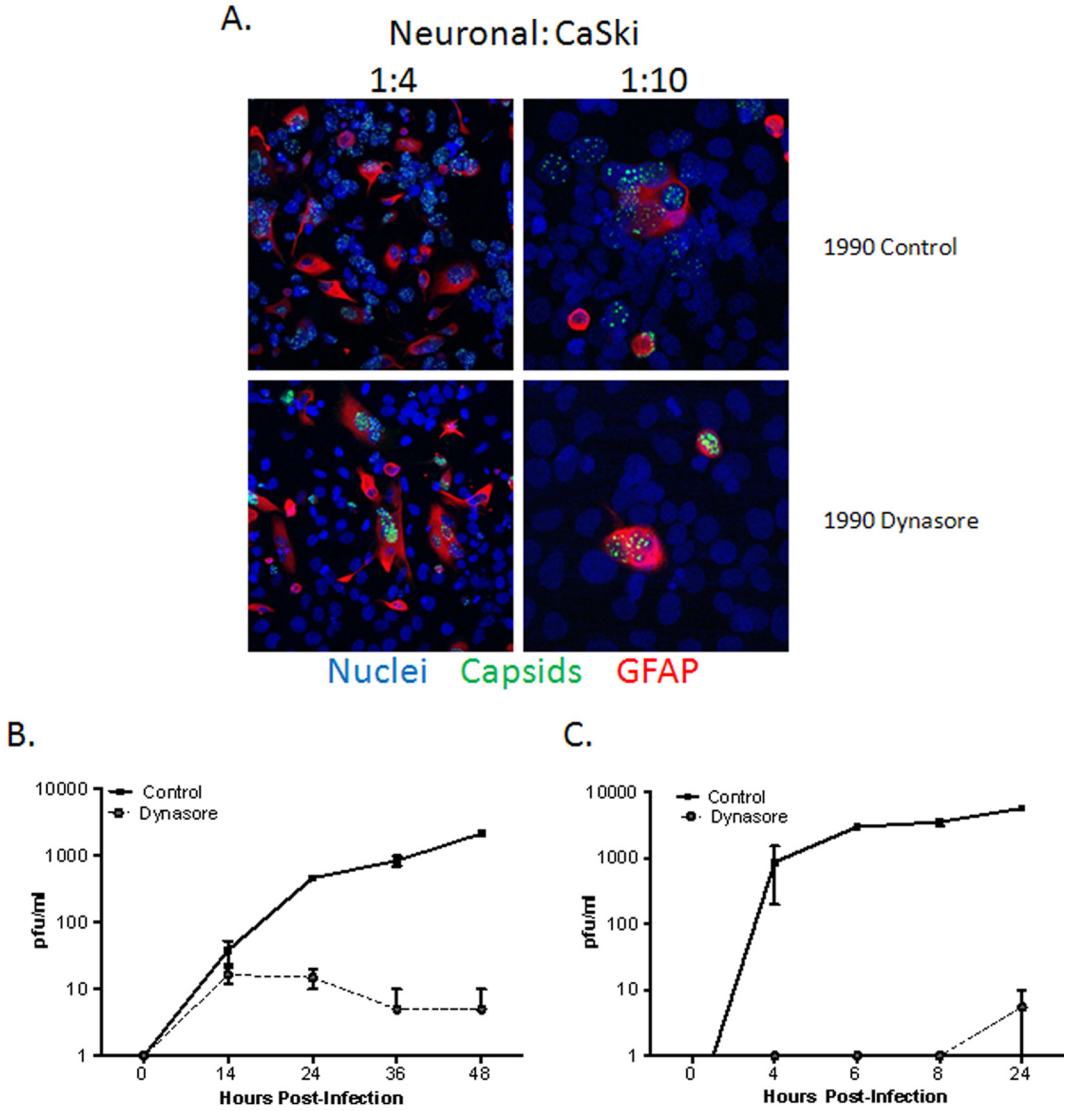

FIG 9 Dynasore prevents cell-to-cell spread. (A) Primary human neuronal cells were infected with HSV-1(KVP26GFP) (10 PFU/cell) for 1 h at 37°C. Then unbound virus was washed off, and cells were trypsinized and cocultured on a layer of untreated CaSki cells (~ 90% confluence) on glass coverslips at a ratio of ~1:4 or 1:10 (infected neuronal cells to uninfected CaSki cells). At 5 h postinfection, dynasore (80 μM in 0.25% DMSO) or a control medium (0.25% DMSO) was added to these cocultures. At 18 h p.i., cells were fixed with 4% paraformaldehyde and were stained with a primary anti-GFAP antibody (red); nuclei were stained with DAPI (blue). Images are representative of 3 independent experiments. 1990, 199V medium supplemented with 0.2% pooled human immunoglobulin (Sigma). (B) One-step growth of HSV-2 was quantified by infecting SK-N-SH cells with an MOI of 5 PFU/cell and adding dynasore or a control buffer to the overlay medium. The culture supernatants were harvested at the indicated times and were diluted 1:10 to decrease any residual dynasore to noninhibitory levels of ≤8 μM. Viral growth was quantified by determining titers on Vero cells. (C) To assess multistep growth, SK-N-SH cells were infected with an MOI of 0.02 PFU/cell, and dynasore or a control buffer was added to the overlay medium 6 h p.i. Culture supernatants were harvested at the indicated times, and titers were determined on Vero cells as for the single-step growth curve. Data shown are from two experiments conducted in duplicate; growth curves are significantly different ($P < 0.001$) by two-way analysis of variance.

namin; inhibition of other GTPases, either by adding ML141, an allosteric inhibitor of Cdc42 GTPase, or by transfecting cells with a dominant negative form of Rac1, had no effect. The latter findings are consistent with an earlier study showing that HSV-1 infection of keratinocytes was independent of pathways involving Rac1 and Cdc42 (38).

Following their synthesis, the capsid proteins localize in the infected-cell nucleus, where capsid assembly occurs. VP5, the major capsid protein, was detected in the nucleus at similar levels in dynasore-treated and control cells when dynasore was added 4 to 8 h postinfection (Fig. 6C and 8), but not in the cytoplasm. These findings suggest that dynasore does not impede the nuclear localization of newly synthesized proteins but rather blocks the transport of the proteins out of the nucleus. Proximity ligation studies demonstrated that VP5 interacts with dynamin (Fig. 7) but is retained in the nucleus in dynasore-treated cells. In agreement with the findings of reduced cytoplasmic VP5 levels, few cytoplasmic or cell surface capsids were detected by electron microscopy when dynasore was added postentry (Fig. 8). The latter observations suggest a defect in capsid assembly and/or a breakdown of nucleus-associated capsids if they are unable to leave the nucleus when dynasore is present.

Only one other study, with vesicular stomatitis virus (VSV), has examined a role for dynamin (and dynasore) post-viral entry. The authors found that the matrix protein of VSV interacted directly with dynamin in coimmunoprecipitation studies and that the addition of dynasore postentry reduced the number of infectious progeny. A similar phenotype was observed when cells were infected with a recombinant virus expressing a mutated form of the matrix protein that did not interact with dynamin; electron microscopy revealed few of the mutant viral particles in the extracellular space, and the G protein was confined to perinuclear vesicles (39).

Together, these studies identify a role for dynamin not only in viral entry but also in the transport of viral proteins and capsids out of the nucleus, thus identifying another cellular pathway usurped by viruses to promote infection. These findings suggest that identifying molecules that specifically block the interactions between dynamin and viral capsid proteins could provide a new target for antiviral therapy.

ACKNOWLEDGMENTS

We thank Brad Poulos, Director of the Human Fetal Tissue Repository, and Joan Berman for providing fetal neuronal cells. We thank the Analytical Imaging Core at Albert Einstein College of Medicine for electron microscopy studies.

This work was supported by grants from the National Institutes of Health (AI065309 [to B.C.H.] and AI083285 [to D.W.W.]) and the Center for AIDS Research at the Albert Einstein College of Medicine and Montefiore Medical Center (NIH AI-051519).

REFERENCES

1. **Wilson SS, Fakioglu E, Herold BC.** 2009. Novel approaches in fighting herpes simplex virus infections. Expert Rev Anti Infect Ther **7:**559–568. http://dx.doi.org/10.1586/eri.09.34.
2. **Xu F, Sternberg MR, Kottiri BJ, McQuillan GM, Lee FK, Nahmias AJ, Berman SM, Markowitz LE.** 2006. Trends in herpes simplex virus type 1 and type 2 seroprevalence in the United States. JAMA **296:**964–973. http://dx.doi.org/10.1001/jama.296.8.964.
3. **Freeman EE, Weiss HA, Glynn JR, Cross PL, Whitworth JA, Hayes RJ.** 2006. Herpes simplex virus 2 infection increases HIV acquisition in men and women: systematic review and meta-analysis of longitudinal studies. AIDS **20:**73–83. http://dx.doi.org/10.1097/01.aids.0000198081.09337.a7.
4. **Corey L, Wald A, Patel R, Sacks SL, Tyring SK, Warren T, Douglas JM, Jr, Paavonen J, Morrow RA, Beutner KR, Stratchounsky LS, Mertz G, Keene ON, Watson HA, Tait D, Vargas-Cortes M.** 2004. Once-daily valacyclovir to reduce the risk of transmission of genital herpes. N Engl J Med **350:**11–20. http://dx.doi.org/10.1056/NEJMoa035144.
5. **Celum C, Wald A, Hughes J, Sanchez J, Reid S, Delany-Moretlwe S, Cowan F, Casapia M, Ortiz A, Fuchs J, Buchbinder S, Koblin B, Zwerski S, Rose S, Wang J, Corey L.** 2008. Effect of aciclovir on HIV-1 acquisition in herpes simplex virus 2 seropositive women and men who have sex with men: a randomised, double-blind, placebo-controlled trial. Lancet **371:**2109–2119. http://dx.doi.org/10.1016/S0140-6736(08)60920-4.
6. **Celum C, Wald A, Lingappa JR, Magaret AS, Wang RS, Mugo N, Mujugira A, Baeten JM, Mullins JI, Hughes JP, Bukusi EA, Cohen CR, Katabira E, Ronald A, Kiarie J, Farquhar C, Stewart GJ, Makhema J, Essex M, Were E, Fife KH, de Bruyn G, Gray GE, McIntyre JA, Manongi R, Kapiga S, Coetzee D, Allen S, Inambao M, Kayitenkore K, Karita E, Kanweka W, Delany S, Rees H, Vwalika B, Stevens W, Campbell MS, Thomas KK, Coombs RW, Morrow R, Whittington WL, McElrath MJ, Barnes L, Ridzon R, Corey L.** 2010. Acyclovir and transmission of HIV-1 from persons infected with HIV-1 and HSV-2. N Engl J Med **362:**427–439. http://dx.doi.org/10.1056/NEJMoa0904849.
7. **Watson-Jones D, Weiss HA, Rusizoka M, Changalucha J, Baisley K, Mugeye K, Tanton C, Ross D, Everett D, Clayton T, Balira R, Knight L, Hambleton I, Le Goff J, Belec L, Hayes R.** 2008. Effect of herpes simplex suppression on incidence of HIV among women in Tanzania. N Engl J Med **358:**1560–1571. http://dx.doi.org/10.1056/NEJMoa0800260.
8. **Cheshenko N, Keller MJ, MasCasullo V, Jarvis GA, Cheng H, John M, Li JH, Hogarty K, Anderson RA, Waller DP, Zaneveld LJ, Profy AT, Klotman ME, Herold BC.** 2004. Candidate topical microbicides bind herpes simplex virus glycoprotein B and prevent viral entry and cell-to-cell spread. Antimicrob Agents Chemother **48:**2025–2036. http://dx.doi.org/10.1128/AAC.48.6.2025-2036.2004.
9. **Keller MJ, Tuyama A, Carlucci MJ, Herold BC.** 2005. Topical microbicides for the prevention of genital herpes infection. J Antimicrob Chemother **55:**420–423. http://dx.doi.org/10.1093/jac/dki056.
10. **Patel S, Hazrati E, Cheshenko N, Galen B, Yang H, Guzman E, Wang R, Herold BC, Keller MJ.** 2007. Seminal plasma reduces the effectiveness of topical polyanionic microbicides. J Infect Dis **196:**1394–1402. http://dx.doi.org/10.1086/522606.
11. **Segarra TJ, Fakioglu E, Cheshenko N, Wilson SS, Mesquita PM, Doncel GF, Herold BC.** 2011. Bridging the gap between preclinical and clinical microbicide trials: blind evaluation of candidate gels in murine models of efficacy and safety. PLoS One **6:**e27675. http://dx.doi.org/10.1371/journal.pone.0027675.
12. **Obiero J, Mwethera PG, Wiysonge CS.** 2012. Topical microbicides for prevention of sexually transmitted infections. Cochrane Database Syst Rev **6:**CD007961. http://dx.doi.org/10.1002/14651858.CD007961.pub2.
13. **Arii J, Uema M, Morimoto T, Sagara H, Akashi H, Ono E, Arase H, Kawaguchi Y.** 2009. Entry of herpes simplex virus 1 and other alphaherpesviruses via the paired immunoglobulin-like type 2 receptor alpha. J Virol **83:**4520–4527. http://dx.doi.org/10.1128/JVI.02601-08.
14. **Gianni T, Campadelli-Fiume G, Menotti L.** 2004. Entry of herpes simplex virus mediated by chimeric forms of nectin1 retargeted to endosomes or to lipid rafts occurs through acidic endosomes. J Virol **78:**12268–12276. http://dx.doi.org/10.1128/JVI.78.22.12268-12276.2004.
15. **Cheshenko N, Trepanier JB, Stefanidou M, Buckley N, Gonzalez P, Jacobs W, Herold BC.** 2013. HSV activates Akt to trigger calcium release and promote viral entry: novel candidate target for treatment and suppression. FASEB J **27:**2584–2599. http://dx.doi.org/10.1096/fj.12-220285.
16. **Schmid SL, McNiven MA, De Camilli P.** 1998. Dynamin and its partners: a progress report. Curr Opin Cell Biol **10:**504–512. http://dx.doi.org/10.1016/S0955-0674(98)80066-5.
17. **Rahn E, Petermann P, Hsu MJ, Rixon FJ, Knebel-Morsdorf D.** 2011. Entry pathways of herpes simplex virus type 1 into human keratinocytes are dynamin- and cholesterol-dependent. PLoS One **6:**e25464. http://dx.doi.org/10.1371/journal.pone.0025464.
18. **Eugenin EA, Berman JW.** 2003. Chemokine-dependent mechanisms of leukocyte trafficking across a model of the blood-brain barrier. Methods **29:**351–361. http://dx.doi.org/10.1016/S1046-2023(02)00359-6.
19. **Eugenin EA, Berman JW.** 2007. Gap junctions mediate human immunodeficiency virus-bystander killing in astrocytes. J Neurosci **27:**12844–12850. http://dx.doi.org/10.1523/JNEUROSCI.4154-07.2007.
20. **Eugenin EA, D'Aversa TG, Lopez L, Calderon TM, Berman JW.** 2003. MCP-1 (CCL2) protects human neurons and astrocytes from NMDA or HIV-tat-induced apoptosis. J Neurochem **85:**1299–1311. http://dx.doi.org/10.1046/j.1471-4159.2003.01775.x.
21. **Desai P, Person S.** 1998. Incorporation of the green fluorescent protein into the herpes simplex virus type 1 capsid. J Virol **72:**7563–7568.
22. **Antinone SE, Smith GA.** 2010. Retrograde axon transport of herpes simplex virus and pseudorabies virus: a live-cell comparative analysis. J Virol **84:**1504–1512. http://dx.doi.org/10.1128/JVI.02029-09.
23. **Cheshenko N, Del Rosario B, Woda C, Marcellino D, Satlin LM, Herold BC.** 2003. Herpes simplex virus triggers activation of calcium-signaling pathways. J Cell Biol **163:**283–293. http://dx.doi.org/10.1083/jcb.200301084.
24. **Cheshenko N, Trepanier JB, Segarra TJ, Fuller AO, Herold BC.** 2010. HSV usurps eukaryotic initiation factor 3 subunit M for viral protein translation: novel prevention target. PLoS One **5:**e11829. http://dx.doi.org/10.1371/journal.pone.0011829.
25. **Cheshenko N, Herold BC.** 2002. Glycoprotein B plays a predominant role in mediating herpes simplex virus type 2 attachment and is required for entry and cell-to-cell spread. J Gen Virol **83:**2247–2255.
26. **Cheshenko N, Liu W, Satlin LM, Herold BC.** 2007. Multiple receptor interactions trigger release of membrane and intracellular calcium stores critical for herpes simplex virus entry. Mol Biol Cell **18:**3119–3130. http://dx.doi.org/10.1091/mbc.E07-01-0062.
27. **WuDunn D, Spear PG.** 1989. Initial interaction of herpes simplex virus with cells is binding to heparan sulfate. J Virol **63:**52–58.
28. **Barrias ES, Reignault LC, De Souza W, Carvalho TM.** 2010. Dynasore,

a dynamin inhibitor, inhibits *Trypanosoma cruzi* entry into peritoneal macrophages. PLoS One **5:**e7764. http://dx.doi.org/10.1371/journal.pone.0007764.

29. **Permanyer M, Ballana E, Badia R, Pauls E, Clotet B, Este JA.** 2012. Trans-infection but not infection from within endosomal compartments after cell-to-cell HIV-1 transfer to $CD4^+$ T cells. J Biol Chem **287:**32017–32026. http://dx.doi.org/10.1074/jbc.M112.343293.
30. **Hill TA, Odell LR, Quan A, Abagyan R, Ferguson G, Robinson PJ, McCluskey A.** 2004. Long chain amines and long chain ammonium salts as novel inhibitors of dynamin GTPase activity. Bioorg Med Chem Lett **14:**3275–3278. http://dx.doi.org/10.1016/j.bmcl.2004.03.096.
31. **Lee RC, Hapuarachchi HC, Chen KC, Hussain KM, Chen H, Low SL, Ng LC, Lin R, Ng MM, Chu JJ.** 2013. Mosquito cellular factors and functions in mediating the infectious entry of chikungunya virus. PLoS Negl Trop Dis **7:**e2050. http://dx.doi.org/10.1371/journal.pntd.0002050.
32. **Zhu YZ, Xu QQ, Wu DG, Ren H, Zhao P, Lao WG, Wang Y, Tao QY, Qian XJ, Wei YH, Cao MM, Qi ZT.** 2012. Japanese encephalitis virus enters rat neuroblastoma cells via a pH-dependent, dynamin and caveola-mediated endocytosis pathway. J Virol **86:**13407–13422. http://dx.doi.org/10.1128/JVI.00903-12.
33. **Schulz WL, Haj AK, Schiff LA.** 2012. Reovirus uses multiple endocytic pathways for cell entry. J Virol **86:**12665–12675. http://dx.doi.org/10.1128/JVI.01861-12.
34. **Mulherkar N, Raaben M, de la Torre JC, Whelan SP, Chandran K.** 2011. The Ebola virus glycoprotein mediates entry via a non-classical dynamin-dependent macropinocytic pathway. Virology **419:**72–83. http://dx.doi.org/10.1016/j.virol.2011.08.009.
35. **Miyauchi K, Kim Y, Latinovic O, Morozov V, Melikyan GB.** 2009. HIV enters cells via endocytosis and dynamin-dependent fusion with endosomes. Cell **137:**433–444. http://dx.doi.org/10.1016/j.cell.2009.02.046.
36. **Pelchen-Matthews A, Parsons IJ, Marsh M.** 1993. Phorbol ester-induced downregulation of CD4 is a multistep process involving dissociation from $p56^{lck}$, increased association with clathrin-coated pits, and altered endosomal sorting. J Exp Med **178:**1209–1222. http://dx.doi.org/10.1084/jem.178.4.1209.
37. **Devadas D, Koithan T, Diestel R, Prank U, Sodeik B, Dohner K.** 2014. Herpes simplex virus internalization into epithelial cells requires Na^+/H^+ exchangers and p21-activated kinases but neither clathrin- nor caveolin-mediated endocytosis. J Virol **88:**13378–13395. http://dx.doi.org/10.1128/JVI.03631-13.
38. **Petermann P, Haase I, Knebel-Morsdorf D.** 2009. Impact of Rac1 and Cdc42 signaling during early herpes simplex virus type 1 infection of keratinocytes. J Virol **83:**9759–9772. http://dx.doi.org/10.1128/JVI.00835-09.
39. **Raux H, Obiang L, Richard N, Harper F, Blondel D, Gaudin Y.** 2010. The matrix protein of vesicular stomatitis virus binds dynamin for efficient viral assembly. J Virol **84:**12609–12618. http://dx.doi.org/10.1128/JVI.01400-10.